Raman spectroscopy investigation on amorphous polyetherketoneketone (PEKK)

Karl Delbé, France Chabert

Graphical Abstract

Raman Spectroscopy Investigation on Amorphous Polyetherketoneketone (PEKK)

Karl Delbé,France Chabert

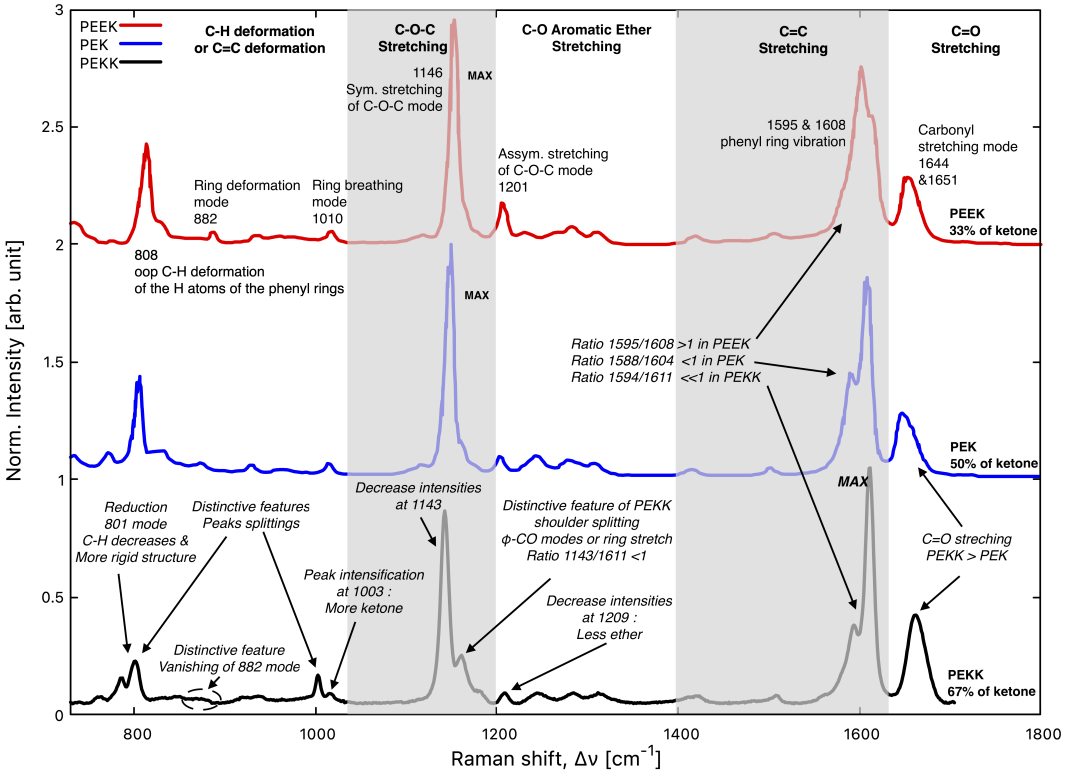

Highlights

Raman Spectroscopy Investigation on Amorphous Polyetherketoneketone (PEKK)

Karl Delbé,France Chabert

- The conditions required to obtain an exploitable Raman spectrum of amorphous PEKK are highlighted.
- We proposed assigning vibrational modes recorded from a hundred spectra on amorphous PEKK. Modes, doublets and intensity ratios are specific to PEKK and distinguish it from other PAEK.
- The ratio of two-thirds ketone to one-third ether in PEKK leads to amplifying the peaks associated with the ketone moiety and a decrease in those associated with the ether moiety compared with PEEK and PEK.

Raman Spectroscopy Investigation on Amorphous Polyetherketoneketone (PEKK)

Karl Delbé[a,*], France Chabert[a]

[a]Laboratoire Génie de Production (LGP), Université de Toulouse, INP-ENIT, 47 avenue d'Azereix, Tarbes, 65000, Occitanie, France

ARTICLE INFO

Keywords:
PEKK
Raman spectroscopy
assignation

ABSTRACT

We used Raman spectroscopy to analyze amorphous polyetherketoneketone (PEKK) and identified the conditions to obtain this material's exploitable Raman spectrum. Our study assigns the vibrational modes observed from 100 spectra recorded on the amorphous PEKK's surface, obtained by injection moulding. The peaks recorded on this polymer are specific to its amorphous microstructure. The vibration modes are similar to PEK and PEEK since they belong to the same family of materials, the polyaryletherketones. However, PEKK has a unique molecular structure with a ketone content of 67% and an ether content of 33%, resulting in an amplification or appearance of vibration modes associated with the ketone group's vibrations and a decrease in the modes related to the ether group. This work provides a valuable database for those studying the microstructure of PEKK and its evolution with processing conditions and ageing.

1. Introduction

Polyaryletherketones (PAEKs) are semi-crystalline high-performance thermoplastic polymers. They demonstrate high-temperature stability, resistance to hydrolysis and most organic chemicals. They keep their high mechanical strength over a wide temperature range, with eventually an operating temperature above 250°C. Due to their outstanding properties, they are considered in many applications: In aerospace, PAEKs replace metals to lighten structures when associated with carbon fibres in composites [1]. Their biocompatibility and durability make them suitable for producing dental or orthopaedic prostheses, offering an alternative option to metal with properties that are closer to the human body[2, 3, 4]. PAEKs are also used as coating layers to reduce wear under friction conditions, including in harsh conditions [5, 6].

Their backbones consist of rigid monomers containing alternately ketone (R-CO-R) and ether groups (R-O-R). The linking group R between the functional groups consists of a 1,4-substituted aryl group. An aryl group is a functional group derived from substituting a hydrogen atom in an aromatic ring compound. Examples of these polymers include polyetherketone (PEK), polyetheretherketone (PEEK) or polyetherketoneketone (PEKK). The ranges of their chemical formulae are displayed in Figure 1.

PAEK can be processed using typical thermoplastic processes, such as injection moulding, extrusion, compression moulding, and additive manufacturing. Additionally, PAEK parts can be welded together [7] or to any thermoplastic part, provided the two polymers are miscible [8].

PEEK, launched by Victrex company in the 80s, is the most used polymer within the PAEK family. The uses of PEEK have gained attention in various industrial applications where it has proven to perform well and last. Besides, its structure and properties have been extensively studied in the scientific literature. Newly, PEKK has emerged on the market, offering mechanical properties similar to PEEK, and higher thermal transitions resulting in stronger heat resistance, due to an additional ketone group as shown in Figure 1. Moreover, the main interest of PEKK lies in slower crystallization kinetics than PEEK, making it easier to control its properties for specific applications [9, 10]. Its wear resistance is also superior to that of PEEK under similar conditions [11, 12]. Although PEKK is not yet as widely used as PEEK, the knowledge on processing-chemical structure-properties relationships is currently making significant progress, as revealed by the increasing number of articles in the literature [6, 13, 14, 15]. Moreover, PEKK can be reinforced with carbon or glass fibres, mica or any fillers to tune its mechanical and tribological properties, with target applications in aerospace structural components [14, 16, 17]. Its ability to osteointegration makes it a strong contender

*Corresponding author
karl.delbe@enit.fr (K. Delbé); france.chabert@enit.fr (F. Chabert)
ORCID(s): 0000-0002-8503-2671 (K. Delbé); 0000-0001-6309-4372 (F. Chabert)

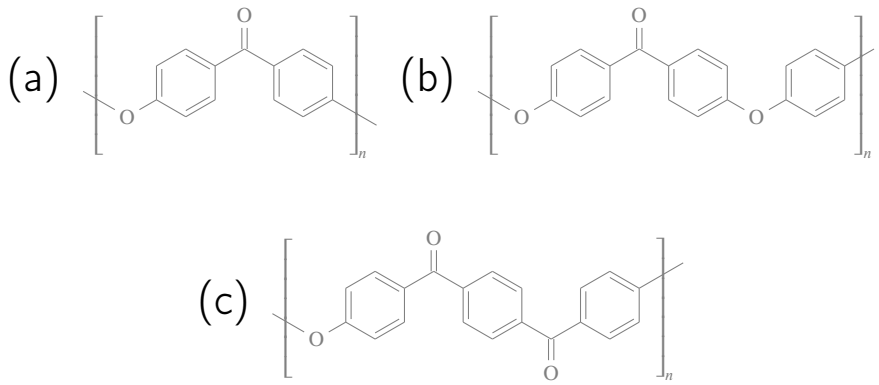

Figure 1: Chemical structure of (a) PEK, (b) PEEK, and (c) PEKK

for dental and cardiovascular applications and joint replacements [18]. The thermal and mechanical properties of PEKK are well-identified, with a melting point of 300 °C and a glass transition at 190 °C [10]. Similar to any thermoplastic materials, the properties of PEKK differ according to its crystallinity, χ_c. The crystallinity and crystallization kinetics depend on the proportion of terephthalic or isophthalic acid units, the T/I ratio (Fig. 2). The elastic modulus of PEKK is slightly higher than PEEK, and its mechanical and thermal characteristics can be controlled by manipulating the T/I ratio when selecting the monomers. Using a specific PEKK grade, it is possible to adjust its crystallinity through fine control of the cooling ramp or annealing conditions while processing [9, 10, 14, 17, 19, 20, 21].

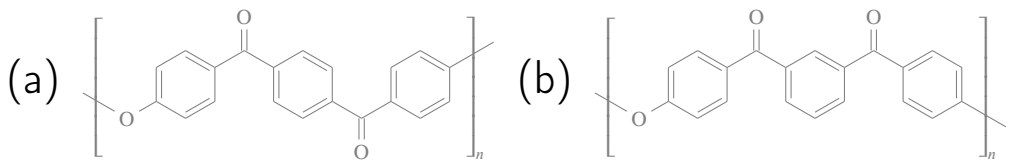

Figure 2: Chemical structure of (a) terephthalic and (b) isophthalic acids

Raman spectroscopy is a powerful and promising non-destructive technique to better understand the local chemical structure of materials. Raman spectroscopy can be useful in characterizing materials such as PEKK. In particular, Raman spectroscopy is an essential tool to analyze polymer surfaces and their evolution with surface treatment, coating or ageing. To do this, tables reporting the assignment of each spectrum peak are necessary. However, such tables on PEKK cannot be found in the literature, probably due to the novelty of polyetherketoneketone in the market. The only research that mentions Raman spectroscopy on PEKK is for dental implants. The authors used Raman scattering analysis, but the study focuses on the ceramic rather than the polymer itself [22]. In addition, some studies on PEEK are valued to gain knowledge on the attribution of PEKK peaks. These studies reveal that Raman spectroscopy allows evaluating their crystallinity [20, 23]. Raman spectroscopy is also used to identify the action of a solvent on the microstructure of PEEK [24], to quantify the evolution of stresses at the surface of a PEEK sample [25] or to evaluate the evolution of the microstructure under the effect of friction [26]. However, one obstacle to using conventional Raman spectroscopy with PAEK is the persistent and prohibitive fluorescence that appears. Fourier transforms spectroscopy generally reduces fluorescence significantly [5]. However, such an approach has not been reported on PEKK until now.

With infrared spectroscopy conducted on PEKK, Lee et al. indicate that the mid-frequency region houses the maximum number of peaks [4]. By studying the vibration modes of PEKK, Pedroso et al. have subdivided the mid-frequency region into specific areas [11]. From 650 cm^{-1} to 1050 cm^{-1}, they observe the C=C deformation modes in benzene rings, followed by C-O-C ether modes from 1100 cm^{-1} to 1300 cm^{-1}. Then, the C=C stretching in benzene rings is located from 1400 to 1600 cm^{-1}, and at approximately 1650 cm^{-1}, they identify the characteristic mode of C=O stretching in the ketone's carbonyl group. Another mode at a high wavenumber, about 3070 cm^{-1}, has also been observed by Mazur et al. in the PEKK's infrared spectroscopy [27].

Table 1
Enthalpies and thermal transitions from DSC experiments with PEKK.

			First heating scan	Cooling	Second heating time
T_g	(°C)	±2 °C	160	162	162
T_{cc}	(°C)	±2 °C	210	-	-
T_{cm}	(°C)	±2 °C	-	290	-
T_m	(°C)	±2 °C	336	-	336
ΔH_m	(J/g)	±2 J/g	32	-	33
ΔH_{cc}	(J/g)	±2 J/g	27	-	-
ΔH_c	(J/g)	±2 J/g	-	32	-
$\chi_{c_{max}}$	(%)		3.8	24	25

In this article, we provide a spectroscopic study of amorphous PEKK with detailed information about the spectrometer, acquisition protocol of the spectra, and post-processing. The section 2 presents the spectra obtained for the PEKK and a proposal for assigning the vibration modes. Finally, perspectives for future works are provided in sections 4 and 5.

2. Material and method

2.1. Amorphous PEKK samples

Kepstan® PEKK grade 7002 is supplied by Arkema France in pellets. PEKK 7002 is a semi-crystalline thermoplastic with tunable crystallinity due to its crystallization kinetics. Its I/T ratio, i.e. the ratio of the terephthalic/isophthalic group, is 70/30. [14]. After drying the pellets at 120 °C for 30 hours, $2 \times 95 \times 95$ mm^3 plates were manufactured with an injection moulding machine Proxima 50 from Billion. The screw-to-nozzle temperatures are regulated from 330 to 370 °C. The mould is kept at 70 °C by oil circulation linked to a cooling bath. The cooling time is 30 s, it is fast enough to obtain amorphous PEKK, as revealed by the optical transparency of the plates. Differential Scanning Calorimetry (DSC) scans were carried out in a DSC 1 Stare System Mettler Toledo to check crystallinity. Samples of 8 to 10 mg were cut into the PEKK plates, experiments were repeated 5 times. Ramps of 10 K.min^{-1} were used for heating from 25 °C to 380 °C, and cooling from 380 ºC to 25 ºC. Glass transition temperature (T_g), melting temperature (T_m), cold crystallization temperature (T_{cc}) and crystallinity (χ_c) were obtained on heating. Cooling ramps were used to obtain the crystallization temperature from melt (T_{cm}) and the maximum crystallinity ($\chi_{c_{max}}$). The melting enthalpy ΔH_m is calculated from the melting peak area divided by the theoretical melting enthalpy of the PEKK if 100% crystalline [20]. However, this value is unknown due to the novelty of the polymer. For this reason, it is commonly assumed that the reference is the PEEK for which $\Delta H_{100\%} = 130$ J/g [28]. The crystallization enthalpy measured on the first heating scan ΔH_c and the crystallization enthalpy measured on cooling is ΔH_{cc}. All the enthalpies calculated and the thermal transitions from the experimental runs are gathered in table 1.

From these data, the initial degree of crystallinity of the injected plates is 3.8%, whereas the maximum crystallinity that PEKK could reach is 25%. This quasi-amorphous state stems from the fast cooling that the plates undergone during injection moulding. Indeed, it is well known that the crystallinity is correlated to the cooling kinetics. When injecting in the mould regulated at 70 °C, the macromolecules do not have enough time to self-organize into lamellae, resulting in a quasi-amorphous polymer. For all the so-injected plates, the crystallinity ranges from 0 to 4%. Moreover, considering the injection moulding process, the specimen surface is cooled faster than inside the part, giving the well-known skin-core defect. When cutting the DSC samples, the surface and the core are taken together, and the crystallinity measured is averaged. The penetration thickness of the beam in Raman spectroscopy is about one micrometre, according to the acquisition conditions. Thus, we consider the crystallinity of the PEKK surface to be close to 0%. Raman spectra are registered on the PEKK plate surface.

2.2. Raman spectrometer

We used a Renishaw spectrometer, the Qontor InVia. It is equipped with a 785 nm wavelength and 300 mW power laser. The beam is directed onto the sample using a Leica DM2700 optical microscope specially adapted to the spectrometer. The spectra were recorded under the following conditions unless stated otherwise. The objective used is a ×100. The working distance is 0.27 mm, and the numerical aperture is 0.85. The slit is 65 µm wide. An Edge filter eliminates Rayleigh scattering up to 50 cm^{-1}. The holographic grating has 1200 lines per mm, giving a spectral

resolution of 1.1 cm^{-1}. The detector is a Renishaw Centrus 2NA000 CCD with 1040 × 256 pixels and is cooled by the Peltier effect.

Given the chosen conditions, the laser's lateral resolution is 1.13 µm, and the field depth is Δz=1.09 µm. For this study, ten spectra were recorded over ten different areas of the sample, scanning the grating over a wide spectral range, between 50 cm^{-1} and 3250 cm^{-1} with an exposure time of 10 seconds and 10 accumulations. Figure 3 shows an average of these ten spectra. The other spectra in Figures 4, 6 and 7 are extracted from acquisitions taken under the following conditions: 100 spectra were recorded on the surface of the amorphous PEKK sample over an area of 500 µm × 500 µm. Each spectrum is spaced 50 µm apart to ensure the most reliable collection possible. A spectrum is obtained with an exposure time of two seconds with ten integrations. Before and after each spectrum, the visual appearance of the polymer is checked to confirm that no thermal damage has occurred. Spectra are acquired over three different spectral ranges:

- between 50 and 1195 cm^{-1} ;
- between 590 and 1705 cm^{-1} ;
- between 2495 and 3265 cm^{-1}.

The spectra are recorded and post-processed using Wire 5 software. The post-processing consists of subtracting the baseline. Any cosmic peaks are also removed. Finally, the spectrum is normalised to the most intense peak at approximately 1611 cm^{-1}. The peaks are then fitted with a deconvolution using a Voigt function.

3. Results

Figure 3 displays the Raman spectrum of PEKK, which was recorded from 50 cm^{-1} to 3150 cm^{-1}. The fluorescence has not yet been processed, and any cosmic peaks have been erased. The spectrum has been normalised to the sharp, intense peak at approximately 1611 cm^{-1}. It can be observed that fluorescence does not hinder detecting PEKK vibrational modes for similar acquisition conditions. In fact, a spectrum with a low signal/noise ratio, low fluorescence, and sharp peaks can be easily obtained. On the other hand, it is much more difficult to achieve a result of this quality with PEEK under these conditions [5, 20, 23].

We proposed to split the spectrum into three zones:

- the low-frequency region between 50 and 200 cm^{-1};
- the mid-frequency region between 200 and 2000 cm^{-1};
- the high-frequency region above 2000 cm^{-1}.

The assignment of peaks is essentially made with the help of Raman spectroscopy data from the literature on PEEK and PEK, and in particular that of Agbenyega et al. [23] and Ellis et al. [5], from which the table 2 is strongly inspired. The work on PEKK by Lee et al. using infrared spectroscopy also confirms these vibrational mode assignments [4]. Table 2 details the position of each peak obtained after the post-processing and deconvolution.

3.1. Low-frequency region

The continuum background increases significantly in the low-frequency region, between 50 and 200 cm^{-1} (Fig. 4). The proximity of Rayleigh scattering causes this rise in the baseline from the right to the left of the spectrum. In 2021, Yamaguchi et al. recorded spectra of PEEK in this region [29]. They detected two peaks: the first one at 97 cm^{-1} and the second one at 135 cm^{-1}. Inspired by studies of Lipiäinen et al., they associated these peaks with intermolecular vibration modes or phonons [30]. Later, in 2022, Yang et al. carried out molecular dynamics calculations for PEEK below 350 cm^{-1}. They confirmed the phonon hypothesis and clarified the mode assignment. At around 85-98 cm^{-1}, they identified the scissoring of ether moiety. Around 130-145 cm^{-1}, they pinpointed the torsion of the ketone group and the connected benzene rings. At around 175-190 cm^{-1}, they recognised the rotation around the ketone groups. This last mode of vibration depends on the length of the molecule under consideration. It can reach 164-165 cm^{-1} when the molecule is elongated [31].

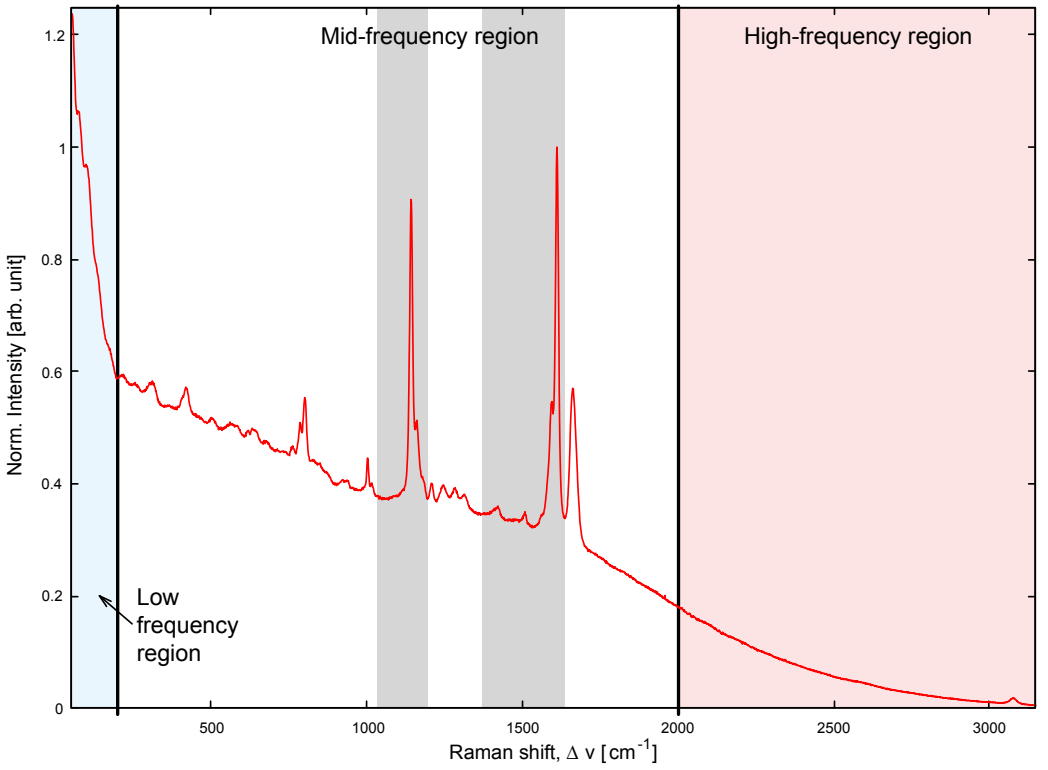

Figure 3: PEKK spectrum recorded between 50 cm^{-1} and 3250 cm^{-1}. The fluorescence has not yet been processed, and any cosmic peaks have been erased. The spectrum is subdivided into three regions: on the left, with a blue background, the low-frequency region; in the centre, the intermediate-frequency region; and on the right, with a red background, the high-frequency region. The central region is split into five domains, alternately coloured between white and grey. Section 3.2 contains the description of each domain's characteristics.

Our PEKK spectra show the presence of three peaks with very weak intensities. These peaks are at 77 cm^{-1}, 109 cm^{-1} and 135 cm^{-1}, respectively. They are lower than those of PEEK mentioned above. The stiffening of the PEKK molecule by the additional ketone group probably lowers the phonon frequencies. The length of the PEKK chain may also be responsible for this lower frequency. It seems appropriate to us to assign the modes at 109 cm^{-1} and 135 cm^{-1} in the manner proposed by Yang et al., i.e. by associating them with intermolecular modes of vibration of the ϕ-O-ϕ and ϕ-CO-ϕ type respectively. The mode at 77 cm^{-1} is also a phonon mode of one of the abovementioned types. An analysis by molecular dynamics would enable it to be assigned without a doubt.

3.2. Mid-frequency region

The mid-frequency region contains the most significant number of peaks (Fig 5). It can also be subdivided according to the molecular groupings that produce the majority of vibrational modes in this region. This separation is similar to that observed using infrared spectroscopy [11]. However, taking into account the work of Ellis et al. [5], we propose a subdivision into five domains:

- between 200 and 1020 cm^{-1}, the out-of-plane C-H deformation of the hydrogen atoms attached to the aromatic rings, γ_{C-H};
- between 1020 and 1200 cm^{-1}, the in-plane C-H deformation of the hydrogen atoms attached to the aromatic rings, δ_{C-H} and C-O-C stretching ;
- between 1200 and 1540 cm^{-1}, stretching of C-O or C-O-C bonds, ν_{C-O} or ν_{C-O-C};
- between 1540 and 1635 cm^{-1}, the stretching vibration of the C=C ring, $\nu_{C=C}$;

Table 2
Wavenumbers and assignments for PEEK, PEK from [5, 24] and PEKK.γ: out-of-plane shear strain; δ: in-plane shear strain; ν: stretching. The peak at 1611 represents 100% intensity. *vw*: very weak intensity, less than 2%; *w*: weak, between 2% and 5%; *m*: medium, between 5% and 15%; *s*: strong, between 15% and 50%; *vs*: very strong, above 50%. *sh* is a shoulder.

PEEK		PEK		PEKK		Assignment
$\Delta\nu$ (cm^{-1})		$\Delta\nu$ (cm^{-1})		$\Delta\nu$ (cm^{-1})		
				77	*vw*	phonon
97	*vw*			109	*vw*	phonon ϕ-O-ϕ
135	*vw*			135	*vw*	phonon ϕ-CO-ϕ
632	*w, sh*	635	*w*	632	*w*	γ_{-CO-} ou δ_{ϕ} ip
646	*w*	647	*vw, sh*	647	*w, sh*	γ_{C-H}
669	*w*	668	*w*			γ_{C-H}
680	*vw*	679	*w*	677	*vw*	γ_{C-H}
731	*vw*	732	*w*	727	*vw*	γ_{C-H}
772	*w*	771	*w*	761	*w*	γ_{C-H}
				786	*m, sh*	γ_{C-H}
808	*s*	802	*s*	801	*s*	γ_{C-H}
825	*w, sh*	830	*w, sh*	830	*w*	γ_{C-H}
882	*w*	872	*w*	871	*vw*	γ_{C-H} or ring mode
932	*w*	927	*w*	920	*w*	γ_{C-H} , or symmetric $\nu_{\phi-CO-\phi}$
934	*vw*	956	*vw*	938	*w*	γ_{C-H}
968	*vw*	972	*vw*	992	*vw, sh*	γ_{C-H}
1010	*vw*	1012	*vw*	1003	*m*	ring stretching mode, or δ_{C-H}
				1017	*w, sh*	ring stretching mode, or δ_{C-H}
1065	*vw*	1064	*vw*			γ_{C-H}
1096	*vw, sh*	1099	*vw, sh*			δ_{ϕ}
1114	*vw*	1115	*vw*			δ_{C-H} or ν_{C-O}
1146	*vs*	1144	*vs*	1143	*vs*	symmetric ν_{C-O-C}
1161	*w, sh*	1159	*sh*	1162	*m, sh*	δ_{C-H} or $\phi - O$ and $\phi - CO$ modes
1173	*w, sh*	1171	*sh*	1178	*w, sh*	δ_{C-H}
1201	*m*	1202	*w*	1209	*m*	$\nu_{\phi-O}$
		1233	*sh*			
		1243	*m*	1246	*w*	asymmetric ν_{C-O-C}
1271	*w*					
1288	*w*	1290	*vw*	1283	*w*	$\nu_{\phi-CO-\phi}$ or ring mode
1307	*w*	1306	*w*	1314	*w*	ring mode
	w			1407	*vw, sh*	$\nu_{C=C}$, ν_{-CO-}, or ν_{C-O-C}
1414	*vw*	1415	*w*	1421	*w*	ν_{-CO-}, ν_{C-O-C}
1499	*vw*	1499	*vw*	1492	*vw, sh*	Ring stretching mode
1576	*w, sh*			1508	*w*	$\nu_{C=C}$
		1588	*m, sh*	1587	*w, sh*	$\nu_{C=C}$
1595	*vs*			1594	*s, sh*	$\nu_{C=C}$
1607	*s, sh*	1604	*vs*	1611	*vs*	$\nu_{C=C}$
1644	*m*	1643	*m*	1658	*m*	$\nu_{C=O}$ crystalline
1651	*m, sh*	1651	*m, sh*	1664	*m, sh*	$\nu_{C=O}$ amorphous
		3063	*sh*			ν_{C-H}
3067	*m*	3069	*m*	3076	w	ν_{C-H}

- between 1635 and 1700 cm^{-1}, stretching of the carbonyl C=O bond in the ketone group $\nu_{C=O}$.

3.2.1. Out-of-plane C-H deformation region

This region contains numerous strong to very weak intensity modes corresponding to out-of-plane deformations of the C-H bond in the phenyl ring [23]. The most prominent peak observed is at 801 cm^{-1} (Fig. 6, left side). In the case of PEKK, this mode is accompanied by two slight shoulders of very weak intensity at 786 cm^{-1} and 761 cm^{-1},

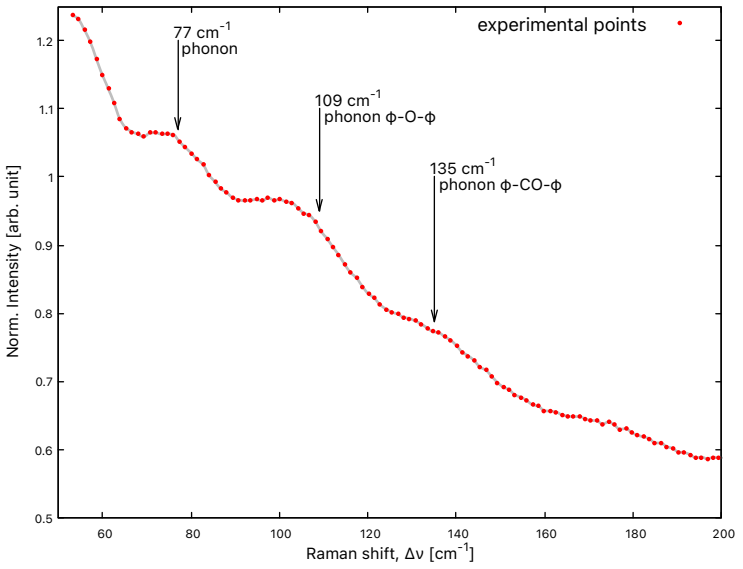

Figure 4: PEKK spectrum in the low-frequency region, between 50 and 200 cm^{-1}. Three peaks at 77, 109 and 135 cm^{-1} are associated with intermolecular interactions, also called phonon modes.

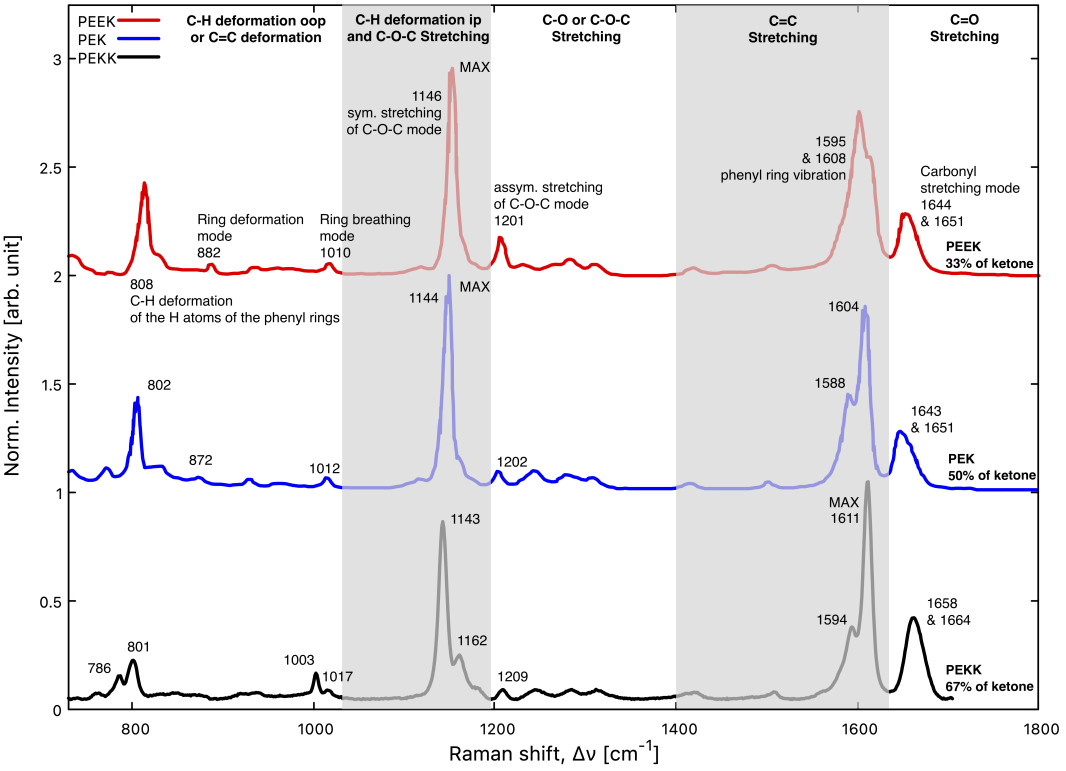

Figure 5: Between 750 and 1700 cm^{-1} are the PEEK (top, red), PEK (middle, blue) and PEKK (bottom, black) spectra.

a distinguishing feature of PEKK that is absent in PEK or PEEK. Furthermore, the intensity of this mode in PEKK is weaker than that in PEK or PEEK. In PEEK and PEK, this mode is located at 808 cm^{-1} and 802 cm^{-1}, respectively.

The ring deformation mode detected around 882 cm^{-1} in PEEK and 872 cm^{-1} in PEK, is also observable at 871 cm^{-1} in PEKK.

Lastly, the mode around 1010 cm^{-1} in PEEK and 1012 cm^{-1} in PEK is split in the PEKK spectrum to form a more intense doublet at 1003 and 1017 cm^{-1}, which is specific to the compound with the highest rate of the ketone.

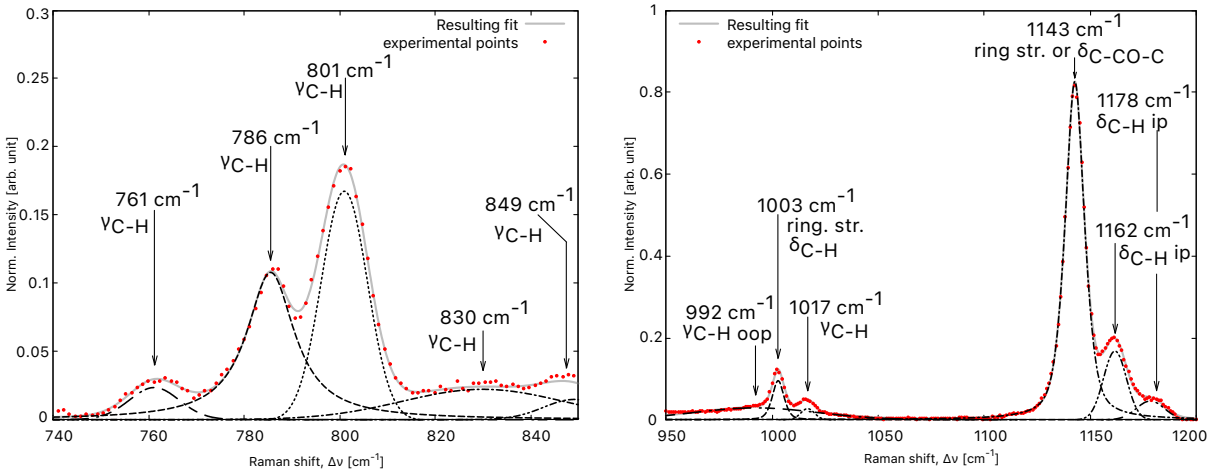

Figure 6: Details of the PEKK spectrum, on the left, between 740 and 850 cm^{-1}, in the γ_{C-H} region, and on the right, between 950 and 1200 cm^{-1}, in the δ_{C-H} region.

3.2.2. In-plane C-H deformation region

The symmetrical C-O-C stretching modes are responsible for the 1143 and 1209 cm^{-1} bands. These bands are the most intense in the PEK and PEEK spectra, as Ellis et al. recorded [5]. In these polymers, the C-O-C stretching mode is also used to normalize the spectra, as it is less sensitive to microstructural variations than other vibration modes [24]. In the case of PEKK, mode at 1143 cm^{-1} is the second most intense after the 1611 cm^{-1} peak.

Additionally, two peaks split at the base of the 1143 cm^{-1} peak, forming a double shoulder of intermediate and weak intensity at 1162 and 1178 cm^{-1} (Fig. 6, right side). This feature is unique to the PEKK spectrum. The mode at 1162 cm^{-1} may be associated with δ_{C-H}, ϕ-O, or ϕ-CO, and the mode at 1178 cm^{-1} is likely related to the δ_{C-H}.

3.2.3. C-O or C-O-C stretching modes region

The modes present in this region are all similar in PEKK, PEEK and PEK. This region contains at 1209 cm^{-1} the antisymmetric counterpart of the strong C-O-C stretching observed in the previous region. This mode is at a lower frequency in PEEK (1201 cm^{-1}) and stronger. The intensity of this mode decreases in PEK. It is weaker in PEKK as the ether group is less concentrated in this compound.

3.2.4. C=C aromatic stretching region

Two very intense modes appear in the spectra of the three materials around 1594 and 1611 cm^{-1} (Fig. 7). In PEEK, Briscoe et al. assign the 1595 mode and its distinct shoulder at 1607 cm^{-1} to phenyl ring vibration [24]. According to Everall et al., these modes depend on the orientation of the laser and its polarization on the sample [32, 33]. They are found at 1594 and 1611 cm^{-1} in PEKK. We note that the 1595/1608 ratio is greater than 1 in the case of PEEK. This ratio is reversed in the case of PEK and PEKK. In PEKK, the 1594 mode is less intense than the 1611 mode. It looks to be a typical feature for materials with a high ketone content. It can be seen that the mode at 1594 cm^{-1} is even weaker in the case of PEKK than in PEK, which may be associated with both the low ether content and the high ketone content.

3.2.5. Carbonyl C=O stretching region

The peaks around 1660 cm^{-1} were also identified on the PEKK IR spectrum around 1651 cm^{-1} [34]. This doublet comprises two vibrational modes at1658 and 1664 cm^{-1}. These peaks appear with the stretching of the carbonyl group, $\nu_{C=O}$. The 1644 and 1651 modes are assigned to the band of C=O stretching. The first is characteristic of the amorphous

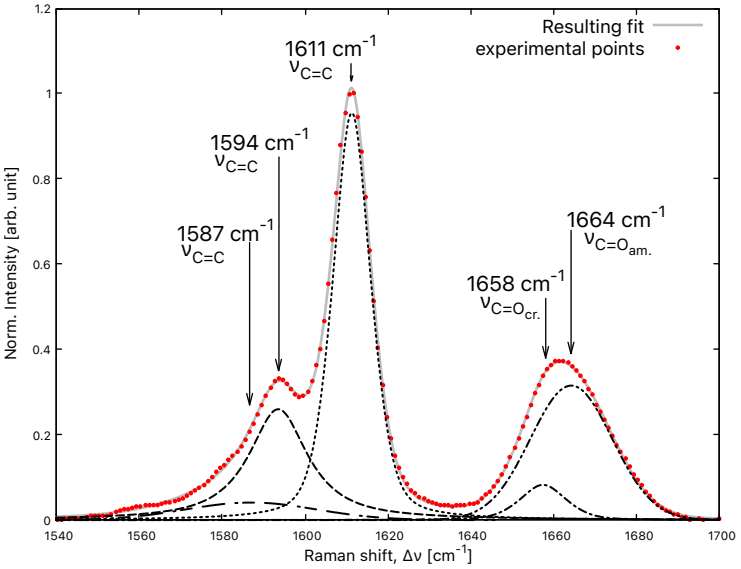

Figure 7: The PEKK spectrum in the mid-frequency region is between 1540 and 1700 cm^{-1}.

structure of PEEK. The latter is relative to the crystalline structure [23]. The same identification is proposed for PEK [5], and we do so for PEKK for the two modes at 1658 and 1664 cm^{-1}. This doublet is more intense in PEKK than in the other two materials. Again, this intensity can be attributed to the high concentration of ketone groups. In our amorphous PEKK spectrum, the intensity of the deconvoluted peak at 1658 cm^{-1} is lower than that of the peak at 1664 cm^{-1}. It would be interesting to compare the evolution of these peaks as a function of the degree of crystallinity to determine whether they can be used as indicators of crystallinity level.

3.3. High-frequency region

Only one mode of vibration has been detected in this region. At 3076 cm^{-1}, a clearly discernible peak with a weak intensity represents C-H bond stretching, ν_{C-H}, attributed by Briscoe et al. for PEEK [24] and also observed in infrared spectroscopy in PEKK by Mazur et al. [27].

4. Discussions

Raman spectroscopy was used to characterize amorphous PEKK. We have proposed assigning the vibrational modes observed from a hundred spectra recorded on the surface of a PEKK specimen. The peaks recorded on this material are characteristic of the amorphous microstructure of PEKK and have an I/T ratio of 70/30. As expected, the vibration modes are similar to those of PEK and PEEK since they belong to the same family of thermoplastic polymers, the PAEK. PEKK differs from the other two in its molecular structure by having a high ketone content of 67% and a low ether content of 33%. This specificity leads to the amplification or the appearance of modes associated with the vibrations of the ketone group. Conversely, there is a decrease in the modes associated with the ether group.

Several aspects distinguish the spectrum of PEKK from those of PEK and PEEK: The mode at 1611 cm^{-1} is the most intense. Alongside this, the shoulder at 1594 cm^{-1} is much weaker than in the case of PEEK. The intensity of the vibration mode in the C=O region is more significant than in PEK and PEEK, corresponding to a higher amount of ketone in the polymer. The increased concentration of ketone favours the appearance of doublets of vibrations: at 1003 and 1017 cm^{-1}, as well as at 786 and 801 cm^{-1} with a lower intensity. Conversely, the fall in ether concentration reduces the intensity of the associated modes, including that at 801 cm^{-1}. Finally, the intensity ratios indicate the ketone concentration, particularly 1611/(1658+1664) and 1594/1611. These intensity ratios effectively distinguished the spectra of PEEK, PEK and PEKK.

The study hereby focuses on amorphous PEKK. These results should be consolidated by a study that takes into account the crystallinity of PEKK. The I/T ratio probably affects the distribution of vibration modes, and a comparative

study that considers this ratio would be a plus for going further into the characterization of this material. Indeed, it would be instructive to check the variation in position, width and intensity ratio of these vibration modes as a function of these two parameters, crystallinity and I/T ratio. The ultimate goal would be to be able to specify for an unknown PAEK, its grade, I/T ratio, and its crystallinity [19, 35]. In the future, Raman spectra of PEKK samples with various crystallinity will be analyzed. The aim is to correlate the Raman peaks with the crystallinity rise. This should make calculating the PEKK samples' crystallinity possible with a fast, accurate, and non-destructive technique.

Like any thermoplastics, the crystallinity correlates with PEKK's properties: density, tensile strength, elastic modulus, toughness, chemical resistance and more. The same applies to the T/I ratio, which plays a role in the crystallization kinetics and physical properties of PEKK. A comparison with other methods for measuring χ_c would provide interesting elements for monitoring crystallinity on the scale of the microscopic probe accessible with modern Raman spectrometers.

Molecular dynamics calculations would be a plus to confirm and complete the attributions proposed in this study, particularly in the low-frequency region, for the mode at 77 cm^{-1}.

5. Conclusions

We studied the Raman spectrum of amorphous PEKK, examining frequencies between 50 and 3250 cm^{-1}. Our research identified phonon vibration modes below 200 cm^{-1} and vibration modes specific to PAEK throughout the rest of the spectrum. By analyzing the vibrational modes, we could differentiate the Raman spectrum of PEKK from PEK and PEEK's. Specifically, we found that the ketone group's high concentration causes specific vibrational modes to intensify, such as the peak at 1611 cm^{-1} or a double shoulder next to the peak at 1143 cm^{-1}. These specific signs are unique to PEKK and are absent in PEEK or PEK. Raman spectroscopy is a valuable tool for characterizing polymers like PEKK. To our knowledge, such analysis does not exist yet in the literature. This data adds to the database of high-performance materials from the PAEK family, making it a valuable resource for future studies.

CRediT authorship contribution statement

Karl Delbé: Conceptualization, Investigation, Writing - Original Draft, Writing - Review Editing, Project administration, Funding acquisition. **France Chabert:** Conceptualization, Investigation, Writing - Review Editing, Funding acquisition.

Acknowledgement

We are grateful to Marcela Matus Aguirre, PhD student at ENIT who injected the specimens. We thank Arkema company for providing the PEKK pellets.

References

[1] Adrian Korycki, Christian Garnier, Margot Bonmatin, Elisabeth Laurent, and France Chabert. Assembling of carbon fibre/peek composites: Comparison of ultrasonic, induction, and transmission laser welding. *Materials*, 15(18):6365, 2022.

[2] Elli Alexakou, Marianna Damanaki, P Zoidis, E Bakiri, N Mouzis, G Smidt, and S Kourtis. Peek high performance polymers: A review of properties and clinical applications in prosthodontics and restorative dentistry. *Eur. J. Prosthodont. Restor. Dent*, 27:113–121, 2019.

[3] Xinglong Hu, Shiqi Mei, Fan Wang, Jun Qian, Dong Xie, Jun Zhao, Lili Yang, Zhaoying Wu, and Jie Wei. Implantable pekk/tantalum microparticles composite with improved surface performances for regulating cell behaviors, promoting bone formation and osseointegration. *Bioactive materials*, 6(4):928–940, 2021.

[4] Wei-Fang Lee, Lu-Ying Wang, Ting-Yi Renn, Jen-Chang Yang, Lih-Sheng Fang, Yi-Huan Lee, and Pei-Wen Peng. Characterization and antibacterial properties of polyetherketoneketone coated with a silver nanoparticle-in-epoxy lining. *Polymers*, 14(14):2906, 2022.

[5] G Ellis, M Naffakh, C Marco, and PJ Hendra. Fourier transform raman spectroscopy in the study of technological polymers part 1: poly (aryl ether ketones), their composites and blends. *Spectrochimica Acta Part A: Molecular and Biomolecular Spectroscopy*, 53(13):2279–2294, 1997.

[6] Anouar El Magri, Sébastien Vaudreuil, Anass Ben Ayad, Abdelhadi El Hakimi, Rabie El Otmani, and Driss Amegouz. Effect of printing parameters on tensile, thermal and structural properties of 3d-printed poly (ether ketone ketone) pekk material using fused deposition modeling. *Journal of Applied Polymer Science*, page e54078, 2023.

[7] Marcella Matus Aguirre, Fabrice Schmidt, France Chabert, André Akué, Rémi Gilblas, Christian Garnier, and Benoît Cosson. Laser transmission welding of pekk: Influence of material properties and process parameters on the weld strength. *Materials Research Proceedings*, 28.

[8] Margot Bonmatin, France Chabert, Gérard Bernhart, Thierry Cutard, and Toufik Djilali. Ultrasonic welding of cf/peek composites: Influence of welding parameters on interfacial temperature profiles and mechanical properties. *Composites Part A: Applied Science and Manufacturing*, 162:107074, 2022.

[9] Sébastien Roland, Mahdi Moghaddam, Sylvie Tencé-Girault, and Bruno Fayolle. Evolution of mechanical properties of aged poly (ether ketone ketone) explained by a microstructural approach. *Polymer Degradation and Stability*, 183:109412, 2021.

[10] L Benedetti, B Brulé, N Decraemer, KE Evans, and O Ghita. Evolution of pekk crystallization measured in laser sintering. *Frontiers in Manufacturing Technology*, 2:964450, 2022.

[11] Judith M Pedroso, Marco Enger, Pedro Bandeira, and Fernão D Magalhães. Comparative study of friction and wear performance of pek, peek and pekk binders in tribological coatings. *Polymers*, 14(19):4008, 2022.

[12] Malik Yahiaoui, France Chabert, J-Y Paris, Valérie Nassiet, and Jean Denape. Friction, acoustic emission, and wear mechanisms of a pekk polymer. *Tribology International*, 132:154–164, 2019.

[13] Xiao-Hua Zhang, Meng-Xiao Jiao, Xin Wang, Bo-Lan Li, Feng Zhang, Yan-Bo Li, Jing-Na Zhao, He-Hua Jin, and Yu Yang. Preheat compression molding for polyetherketoneketone: Effect of molecular mobility. *Chinese Journal of Polymer Science*, 40(2):175–184, 2022.

[14] Helena Perez-Martin, Paul Mackenzie, Alex Baidak, Conchúr M Ó Brádaigh, and Dipa Ray. Crystallinity studies of pekk and carbon fibre/pekk composites: A review. *Composites Part B: Engineering*, 223:109127, 2021.

[15] Miguel Villar, Christian Garnier, France Chabert, Valérie Nassiet, Diane Samélor, Juan Carlos Diez, Andres Sotelo, and Maria A Madre. In-situ infrared thermography measurements to master transmission laser welding process parameters of pekk. *Optics and Lasers in Engineering*, 106:94–104, 2018.

[16] Valentina Donadei, Francesca Lionetto, Michael Wielandt, Arnt Offringa, and Alfonso Maffezzoli. Effects of blank quality on press-formed pekk/carbon composite parts. *Materials*, 11(7):1063, 2018.

[17] Daoji Gan, Shiqiang Lu, Caisheng Song, and Zhijian Wang. Morphologies, mechanical properties and wear of poly (ether ketone ketone)(pekk) and its composites reinforced with mica. *Macromolecular Materials and Engineering*, 286(5):296–301, 2001.

[18] Bo Yuan, Qinwen Cheng, Rui Zhao, Xiangdong Zhu, Xiao Yang, Xi Yang, Kai Zhang, Yueming Song, and Xingdong Zhang. Comparison of osteointegration property between pekk and peek: Effects of surface structure and chemistry. *Biomaterials*, 170:116–126, 2018.

[19] Steven R Lustig, John G Van Alsten, and Benjamin Hsiao. Polymer diffusion in semicrystalline polymers. 1. poly (ether imide)/poly (aryl ether ketone ketone). *Macromolecules*, 26(15):3885–3894, 1993.

[20] Marie Doumeng, Lotfi Makhlouf, Florentin Berthet, Olivier Marsan, Karl Delbé, Jean Denape, and France Chabert. A comparative study of the crystallinity of polyetheretherketone by using density, dsc, xrd, and raman spectroscopy techniques. *Polymer Testing*, 93:106878, 2021.

[21] Marie Doumeng, Florentin Berthet, Karl Delbé, Olivier Marsan, Jean Denape, and France Chabert. Effect of size, concentration, and nature of fillers on crystallinity, thermal, and mechanical properties of polyetheretherketone composites. *Journal of Applied Polymer Science*, 139(5):51574, 2022.

[22] Fei Zhang, Christoph Meyer Zur Heide, Jérome Chevalier, Jozef Vleugels, Bart Van Meerbeek, Christian Wesemann, Bernardo Camargo Dos Santos, Valter Sergo, Ralf-Joachim Kohal, Erik Adolfsson, et al. Reliability of an injection-moulded two-piece zirconia implant with pekk abutment after long-term thermo-mechanical loading. *Journal of the Mechanical Behavior of Biomedical Materials*, 110:103967, 2020.

[23] JK Agbenyega, G Ellis, PJ Hendra, WF Maddams, C Passingham, HA Willis, and J Chalmers. Applications of fourier transform raman spectroscopy in the synthetic polymer field. *Spectrochimica Acta Part A: Molecular Spectroscopy*, 46(2):197–216, 1990.

[24] BJ Briscoe, BH Stuart, PS Thomas, and DR Williams. A comparison of thermal-and solvent-induced relaxation of poly (ether ether ketone) using fourier transform raman spectroscopy. *Spectrochimica Acta Part A: Molecular Spectroscopy*, 47(9-10):1299–1303, 1991.

[25] Kenny Kong, Richard J Davies, Robert J Young, and Stephen J Eichhorn. Molecular and crystal deformation in poly (aryl ether ether ketone) fibers. *Macromolecules*, 41(20):7519–7524, 2008.

[26] Marie Doumeng, Fabrice Ferry, Karl Delbé, Tiphaine Mérian, France Chabert, Florentin Berthet, Olivier Marsan, Valérie Nassiet, and Jean Denape. Evolution of crystallinity of peek and glass-fibre reinforced peek under tribological conditions using raman spectroscopy. *Wear*, 426:1040–1046, 2019.

[27] Rogério L Mazur, Edson C Botelho, Michelle L Costa, and Mirabel C Rezende. Avaliações térmica e reológica da matriz termoplástica pekk utilizada em compósitos aeronáuticos. *Polímeros*, 18:237–243, 2008.

[28] DJ Blundell and BN Osborn. The morphology of poly (aryl-ether-ether- ketone). *Polymer*, 24(8):953–958, 1983.

[29] Makoto Yamaguchi, Shoko Kobayasi, Tomoko Numata, Nobuyuki Kamihara, Toshihiro Shimda, Mitsutoshi Jikei, Mikio Muraoka, Jonathan E Barnsley, Sara J Fraser-Miller, and Keith C Gordon. Evaluation of crystallinity in carbon fiber-reinforced poly (ether ether ketone) by using infrared low frequency raman spectroscopy. *Journal of Applied Polymer Science*, 139(8):51677, 2022.

[30] Tiina Lipiäinen, Sara J Fraser-Miller, Keith C Gordon, and Clare J Strachan. Direct comparison of low-and mid-frequency raman spectroscopy for quantitative solid-state pharmaceutical analysis. *Journal of pharmaceutical and biomedical analysis*, 149:343–350, 2018.

[31] Xiaoran Yang, Seiya Yokokura, Taro Nagahama, Makoto Yamaguchi, and Toshihiro Shimada. Molecular dynamics simulation of poly (ether ether ketone)(peek) polymer to analyze intermolecular ordering by low wavenumber raman spectroscopy and x-ray diffraction. *Polymers*, 14(24):5406, 2022.

[32] NJ Everall, J Lumsdon, JM Chalmers, and N Mason. The use of polarised fourier transform raman spectroscopy in morphological studies of uniaxially oriented peek fibres—some preliminary results. *Spectrochimica Acta Part A: Molecular Spectroscopy*, 47(9-10):1305–1311, 1991.

[33] Abdul G Al Lafi, Ali Alzier, and Abdul W Allaf. Wide angle x-ray diffraction patterns and 2d-correlation spectroscopy of crystallization in proton irradiated poly (ether ether ketone). *Heliyon*, 7(6):e07306, 2021.

[34] Johannes Guenther, Minhao Wong, Hung-Jue Sue, Tim Bremner, and Janet Blümel. High-temperature steam-treatment of pbi, pekk, and a pekk-pbi blend: A solid-state nmr and ir spectroscopic study. *Journal of applied polymer science*, 128(6):4395–4404, 2013.

[35] Chunyu Li and Alejandro Strachan. Prediction of pekk properties related to crystallization by molecular dynamics simulations with a united-atom model. *Polymer*, 174:25–32, 2019.